International Journal of Engineering & Technology, 7 (4.20) (2018) 259-265

International Journal of Engineering & Technology

Website: www.sciencepubco.com/index.php/IJET

Research paper

Finite Element Analysis for The Response of URM Walls Supporting RC Slab

Ammar Rafid Ahmed[1*], Alaa H. Al-Zuhairi[2]

[1]University of Baghdad, Iraq
[2]University of Baghdad, Iraq
**Corresponding author E-mail: ammar.rafid91@gmail.com*

Abstract

The aim for this research is to investigate the effect of inclusion of crack incidence into the 2D numerical model of the masonry units and bonding mortar on the behavior of unreinforced masonry walls supporting a loaded reinforced concrete slab. The finite element method was implemented for the modeling and analysis of unreinforced masonry walls. In this paper, ABAQUS, FE software with implicit solver was used to model and analyze unreinforced masonry walls which are subjected to a vertical load. Detailed Micro Modeling technique was used to model the masonry units, mortar and unit-mortar interface separately. It was found that considering potential pure tensional cracks located vertically in the middle of the mortar and units shows an increase in masonry strength of about 10% than the strength calculated using the procedure recommended by the Masonry Society Joint Committee in the building code.

Keywords: *ABAQUS; Clay Units; Crack Simulation; Detailed Micro Modelling (DMM); Finite Element Method (FEM).*

1. Introduction

Unreinforced masonry (URM) construction is commonly implemented in the construction practices because of its many advantages which consist of good protection to fire, low maintenance, good insulation to thermal and sound and its outstanding durability [1]. The best characteristic of masonry constructions is its simplicity, placing masonry units on top of each other, with or without mortar, is a simple, yet, appropriate practice which has been effective for a very long time [2]. Some examples of masonry assemblies where structural masonry is presently utilized are walls used as load bearing, panels used as infill that is used as diaphragms against wind and seismic loads, pre-stressed masonry as well as low rise structures [2].

The dimensions of masonry units are mostly different from place to another. Many factors influencing masonry strength, such as the strength of units, type of mortar, units and mortar volume. Even though masonry construction has been employed for a very long time, however, for the last four decades or so, the real behavior of masonry structures has been considered and is to be understood completely [3]. The hinder of advanced applications of structural masonry is caused by not developing design procedures to keep up with the developing procedures of concrete and steel [2]. The absence of vision and models that describe the complicated behavior of masonry units, mortar in joints, as well as masonry as a composite material are the fundamental reasons for this hinder [2]. The calculation methods that currently exist are essential of empirical type and the preliminary usage of the tools for the numerical analysis and/or design of masonry constructions [2].

Masonry is a non-homogeneous material that exhibits inelastic and anisotropic behavior and consists of two different materials (units and mortar joints) [4]. Because of the heterogeneity nature of its characteristic and its nonlinear behavior, the modeling and analyzing of masonry structures is challenging [7]. As a result, in order to design masonry constructions, empirical formulas have been utilized.

There are many differences between ancient and modern masonry constructions from modeling and analysis points of view. Ancient masonry construction is a very composite material with three-dimensional inner arrangements, in general, unreinforced nevertheless, may encompass reinforcement. Whereas modern masonry regularly erected in a regular arrangement from masonry units and bonding mortar, steel reinforced or not reinforced. The fact that the inconsistency of the materials which form masonry constructions and the different technologies makes masonry's computational modeling difficult [4].

Nowadays, the presence of innovative numerical tools those are capable of predicting the structural behavior beginning from the linear stage, throughout the course of cracking and degradation until complete strength failure. This goal can be achieved simply through the employment of a precise and robust constitutive model which consequences from the finite element method. Detailed Micro-Modeling (DMM) method is a modern approach of finite element analysis that encompasses distinctly the masonry units and bonding mortar. The DMM technique was firstly presented by "Lourenco, et al. in 1995 [2]" where the representation of masonry units and mortar joints is by continuum solid elements whereas the representation of unit-mortar interface is by discontinuous contact elements [2]. Joints cracking, sliding, units cracking and masonry crushing are the possible failure mechanisms and all must be included in the adopted micro model [6]. Furthermore, the developments of computer hardware allow the applications of sophisticated analysis which permit the structures detailed modeling and the following behavior simulation when exposed to distinctive actions. Even though numerical tools are advancing, it must be incorporated with inno-

vative methods of practices, in other words, a complicated characterization of the model, comprising a detailed representation of the geometry and a huge number of material parameters [7].
Several case studies investigated the factors that affect masonry strength. For example, in India, previous researchers [8] - [11] implemented in their studies mortar relatively stiffer compared to bricks. Conversely, in the western countries, the masonry unit utilized is generally stiffer compared to mortar, Nagarajan, et al. [12] and Gumaste, et al. [13] reported that the non-linear behavior of masonry is mostly mortar responsibility. Hence, the strength of masonry is influenced by unit strength, mortar strength, and its volume.

2. Modeling strategy

Since the mortar joints play an essential role as planes of weakness [6], as a result, distinct directional properties can be found in masonry [14]. The determination of the numerical approach depends on the level of accuracy and the level of simplicity. Units and mortar are modeled separately in the micro modeling technique. There are two types of micro modeling approaches, simplified and detailed micro modeling [15].
The simplified micro modeling technique includes expanded units which are represented by continuum elements while mortar joints and the unit-mortar interface are lumped in discontinuum elements [15]. The DMM approach includes individual simulation of the masonry units and mortar joints by continuum elements whereas the unit-mortar interfaced by discontinuum elements. Considerations of this approach can be found below [15]:

1. The elastic and inelastic properties of both units and mortar.
2. The interface is represented as a potential crack/slip plane with initial dummy stiffness (slave elements) to avoid interpenetration of the continuum (master elements).
3. The combined action of unit, mortar and unit-mortar interface can be examined in this approach under a magnifying glass.

The adopted modeling strategy implemented in this study can be seen in Fig. 1.
In this technique, interface elements permit discontinuities incidence in the displacement field, their behavior is defined depending on the relation between the tractions t and relative displacements u along the interface. The generalized stresses and strains can be written in a linear elastic relation in the standard form as in (1) [2].

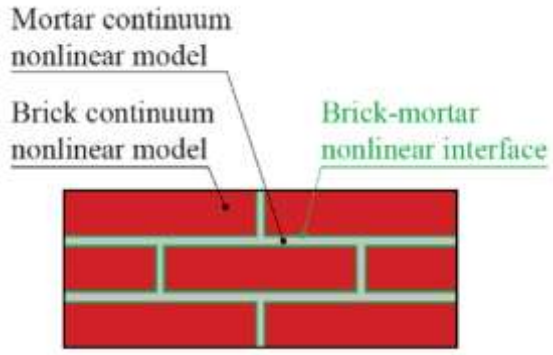

Fig. 1: DMM modeling strategy [16].

$$\sigma = D\varepsilon \tag{1}$$

where, for a 2D configuration
$\sigma = \{\sigma, \tau\}^T$
$D = \begin{bmatrix} k_n & 0 \\ 0 & k_s \end{bmatrix}$
$\varepsilon = \{\Delta u_n, \Delta u_s\}^T$
Where,
n and s = Normal and shear components, respectively.
From the properties of masonry units, bonding mortar, and joint thickness, the elements of elastic stiffness matrix [D] can be found as illustrated in (2) and (3) shown below [3].

$$K_n = \frac{E_u E_m}{h_m (E_u - E_m)} \tag{2}$$

$$K_s = \frac{G_u G_m}{h_m (G_u - G_m)} \tag{3}$$

Where,
E_u and E_m = The Young's moduli for unit and mortar, respectively.
G_u and G_m = The shear moduli for unit and mortar, respectively
h_m = Joint thickness.
A multi-surface model, a composite of yield functions can be used to define the constitutive interface model, as in Fig. 2. This model composed of three separate yield functions associated with softening behavior for the three modes as in (4), (5) and (6) [4].
Tensile criterion:

$$f_t(\sigma, k_t) = \sigma - \bar{\sigma}_t(k_t) \tag{4}$$

Shear criterion:

$$f_s(\sigma, k_s) = |\tau| + \sigma \tan\phi - \bar{\sigma}_s(k_s) \tag{5}$$

Compressive criterion:

$$f_c(\sigma, k_c) = (\sigma^T P \sigma)^{\frac{1}{2}} - \overline{\sigma_c}(k_c \tag{6}$$

Where,
ϕ = The friction angle
P = a projection diagonal matrix, based on material parameters.
$\bar{\sigma}_t$, $\bar{\sigma}_s$ and $\overline{\sigma_c}$,= The isotropic effective stresses of each of the adopted yield functions.
k_t, k_s and k_c = scalar internal variables that affect the isotropic effective stresses.

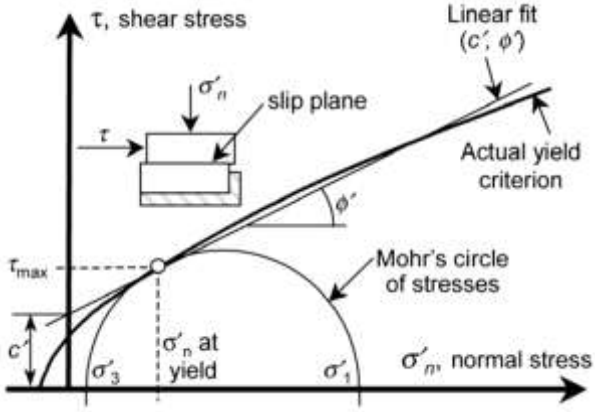

Fig. 2: Mohr-Coulomb Criterion [17].

3. Numerical simulation

The FE software ABAQUS was employed in this study to develop the FE model of clay masonry walls supporting a loaded RC slab. The clay masonry units and mortar joints were modeled using continuum elements while the unit-mortar interface was represented by interaction properties. Potential tensional vertical cracks in the center of the masonry units and mortar joints are modeled as cracks of zero thickness.
In the above-adopted approach, all damages are concentrated in the relatively weak joints and in pure tension potential cracks located vertically in the middle of the units and mortar [18] since cracks are a major source of nonlinear behaviour in masonry [14]. Implicit solver was selected in ABAQUS for modelling and analysing. This method has the capability to simulate linear static loading which was adopted in this study. Masonry units, mortar, and concrete slab were modelled using Continuum Plane Strain 4-noded Reduced Integration CPE4R element. Steel reinforcement was modelled using Truss 2 Dimensional 2-noded T2D2 element. The interface element (i.e. Interaction between units and mortar) was modelled using tangential, normal and cohesive behaviour available in ABAQUS. This model was selected because of its capability to model frictional and cohesive materials, such as granular-like soils and rock [2]. Normal,

tangential, and cohesive behaviour interactions existed in interaction module in ABAQUS were used during the interaction modelling between units and mortar assuming that shear as well as normal forces are transmitted across the interface.

4. Verification of the numerical model

At first, a verification has been conducted by comparing the load-displacement diagram for the numerical model of the masonry prism with the experimental one [19]. The dimensions of the prism were 500 mm high × 240 mm wide × 240 mm thick. The prism consists of 6 courses high and 1 unit across the thickness. The masonry units used to construct the prism are clay brick units of 240 mm ×115 mm × 75 mm and 10 mm thickened mortar used. The geometry of the clay masonry prism and testing setup can be seen in Fig. 3. The prism was subjected to an increased vertical pressure till it reaches failure. The numerical simulation for the FE model of the masonry prism that has been implemented using ABAQUS can be seen in Fig. 4.

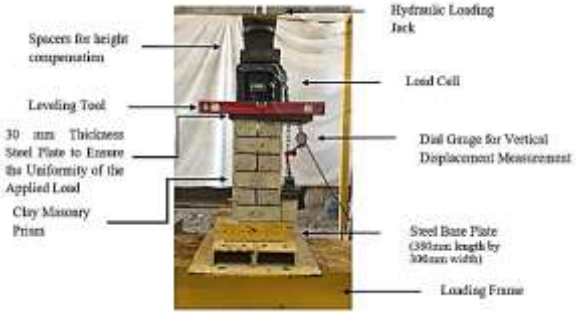

Fig. 3: Test set-up [19].

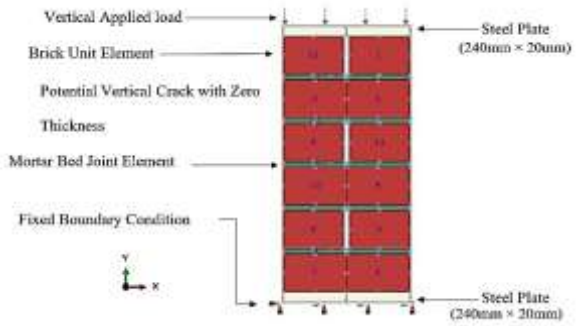

Fig. 4: Numerical simulation of clay masonry prism [19].

Fig. 5 shows that the load-displacement curve of the numerical FE model has almost the same shape and pattern of the load-displacement curve for the experimentally tested prism. In fact, it can be seen that at the beginning of the load application there is a difference in the displacements between the experimental and numerical model. When the pressure is increased to its maximum value, the displacements of both experimental and numerical models reach almost equal values with a difference of about 9%.

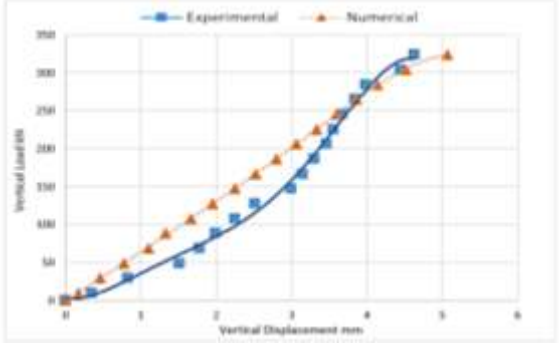

Fig. 5: Load-displacement diagrams of the numerical and experimental results of masonry prism [19].

5. Case study, results and discussion

A 2D model of loaded reinforced concrete slab supported by three URM walls with cracks was simulated using finite element method as shown in Fig. 6. The reinforced concrete slab's dimensions were the 6720mm length and 150mm depth, whereas, the dimensions of the URM walls were 2965mm height × 240mm width and the walls consist of 35 courses bonded by cement mortar as shown in Fig. 7. The walls were constructed using clay masonry units of dimensions 240mm × 115mm × 75mm and cement mortar of 10 mm in thickness. Potential tension vertical cracks with zero thickness were considered at the centre of the masonry units and mortar joints. The pressure was applied as a uniformly distributed compression on the reinforced concrete slab. The bottom tips of the masonry walls were assumed as a pin connected to a rigid footing to prevent any movement in any direction. The applied pressure was increased gradually until it reaches failure, the failure pressure was 1.327 MPa.
The linear (i.e. Modulus of elasticity and Poison's ratio) and non-linear (i.e. angle of internal friction and dilation angle) mechanical characteristics, as well as the compressive and tensile strengths of units, mortar, concrete and steel reinforcement that has been utilized in numerical simulation, are presented in, Tables 1 to 4.

Table. 1: Linear mechanical property of units and mortar [2].

Component	Modulus of elasticity (E_c) (MPa)	Poisson's ratio (υ)
Clay Units	16700	0.15
Cement Mortar	18000	0.10

Table 2: Non-linear mechanical properties of units and mortar [2].

Component	c (MPa)	f_t (MPa)	ϕ	ψ
Clay Units	1.85	1.32	0	36.87
Cement Mortar	0.35	0.25	0	36.87

Where,
c = cohesion.
f_t= tensile strength.
ϕ= angle of internal friction.
ψ= dilation angle.

Table3: Compressive strengths of units and mortar [20].

Material	Compressive strength (MPa)
Brick	13.21
Cement mortar bedding	8.3

Table 4: Linear Mechanical properties of concrete and steel reinforcement.

Component	Modulus of elasticity (E_c) (MPa)	Poisson's ratio (υ)
Concrete	25000	0.2
Steel reinforcement	200000	0.3

The overall deformation of the 2D model under the applied pressure that equals 1.3327 MPa is shown in Fig. 8. As can be seen from the figure below, the deformation of the slab is relatively small compared to the deformation of the URM walls. Also, the direction of the failure starts from the slab towards the supports (i.e. masonry units near the RC slab exhibited failure at the beginning then as the pressure increases the failure continue towards the supports).
Distribution of vertical and horizontal stresses that are generated in masonry units of the walls in x and y directions due to the maximum applied pressure across the length of the wall at different levels of height at interior and exterior walls can be seen in Fig. 9 and Fig. 10, respectively. From these two figures, it can be seen clearly the large difference between the values of horizontal and vertical stresses in masonry units. Consequently, the effect of horizontal stresses in units can be neglected. On the other hand, a little difference can be seen between the stresses in masonry units that consisting the internal and external walls.

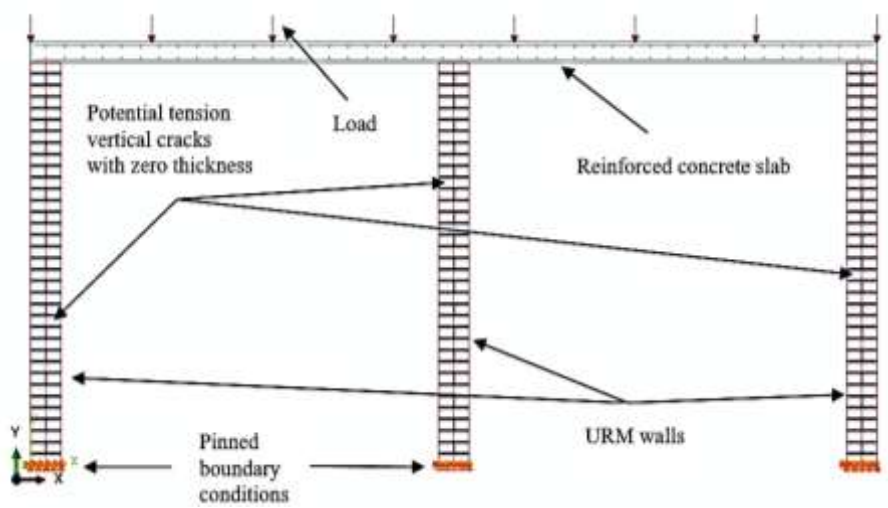

Fig. 6: Modeling of reinforced concrete slab supported by three URM walls.

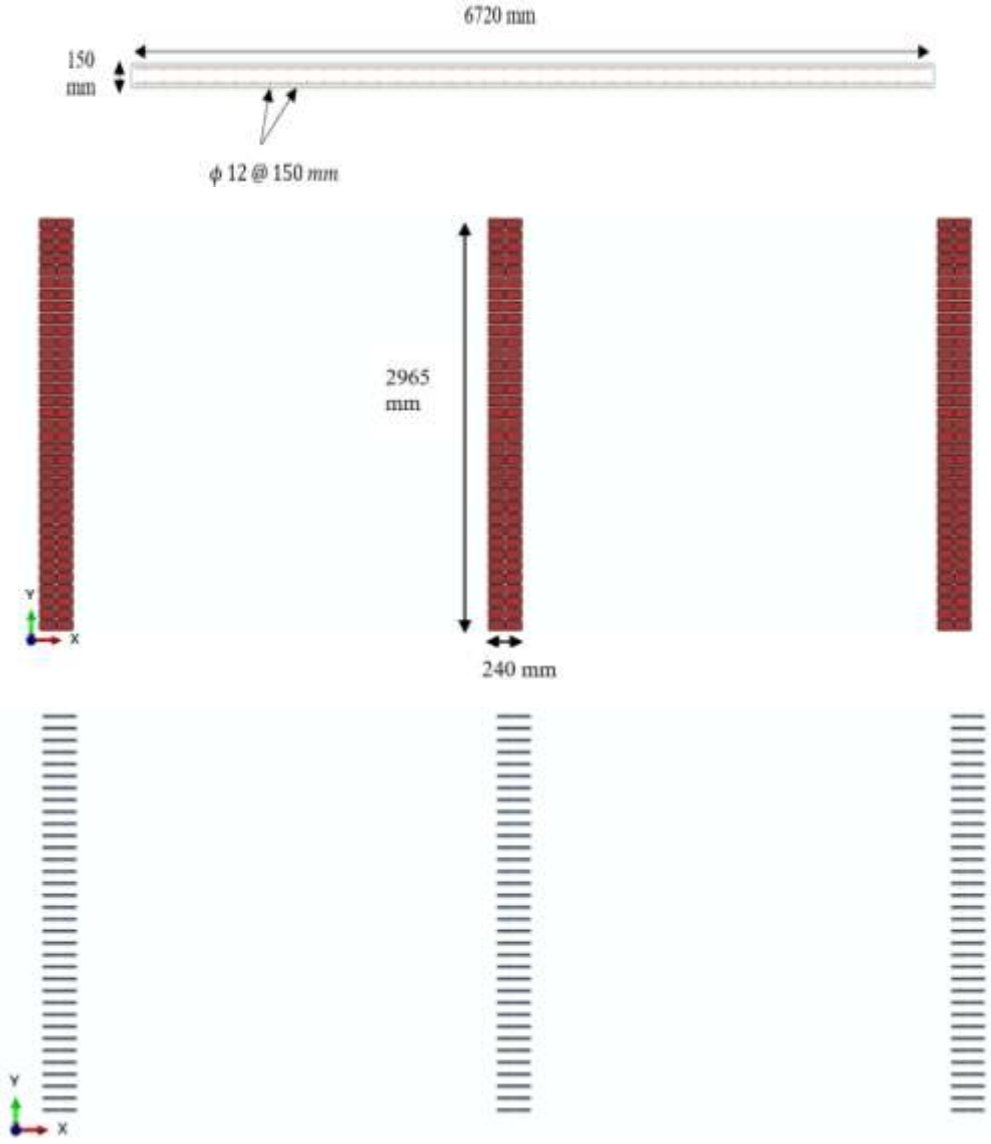

Fig. 7: Geometrical modeling of (a) Reinforced concrete slab (b) URM walls (c) Mortar joints.

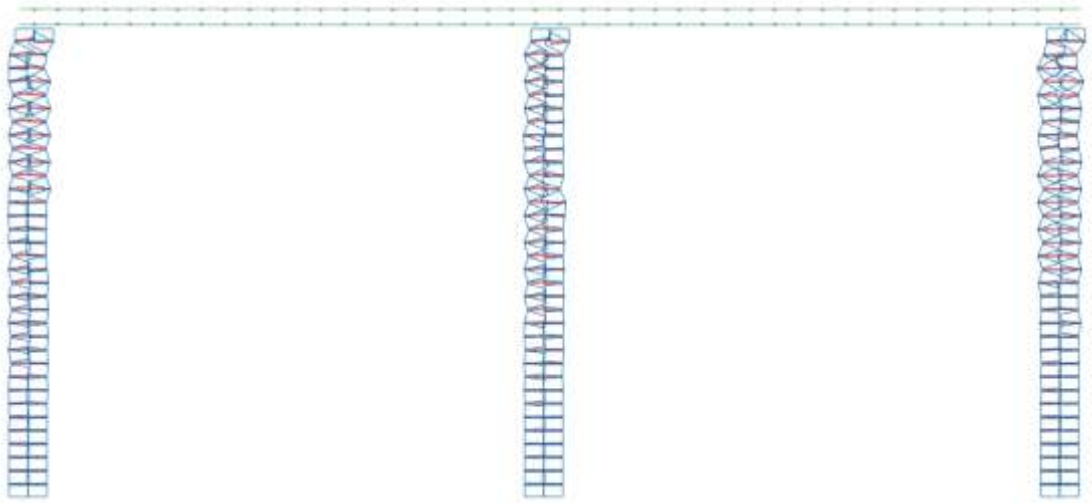

Fig. 8: Overall deformation of the model.

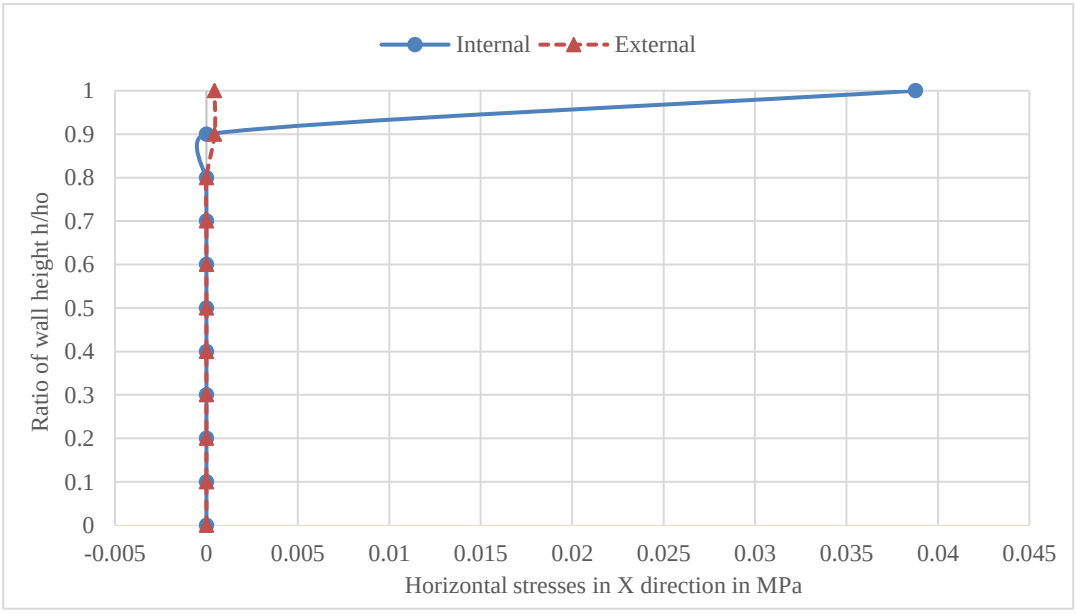

Fig. 9: Generated horizontal stresses in masonry units at the center and edge walls.

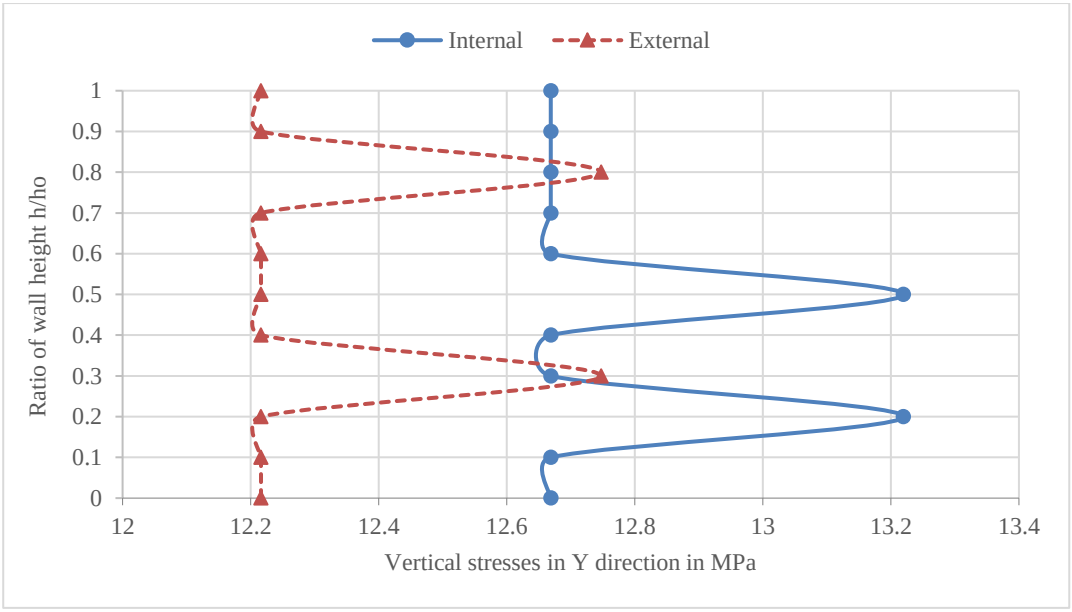

Fig. 10: Generated vertical stresses in masonry units at the center and edge walls.

The illustration of the generated stresses in cement mortar in both directions due to the applied pressure at internal and external walls can be seen in Fig. 11 and Fig.12.

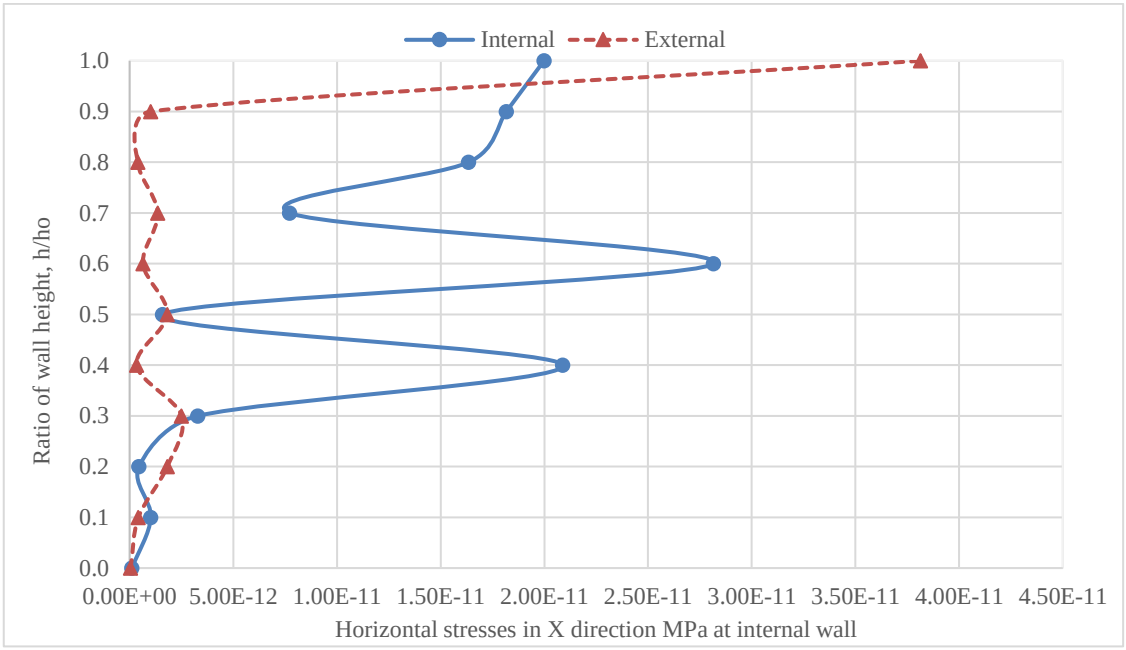

Figure 11: Mortar horizontal stresses in the x-direction at internal and external walls.

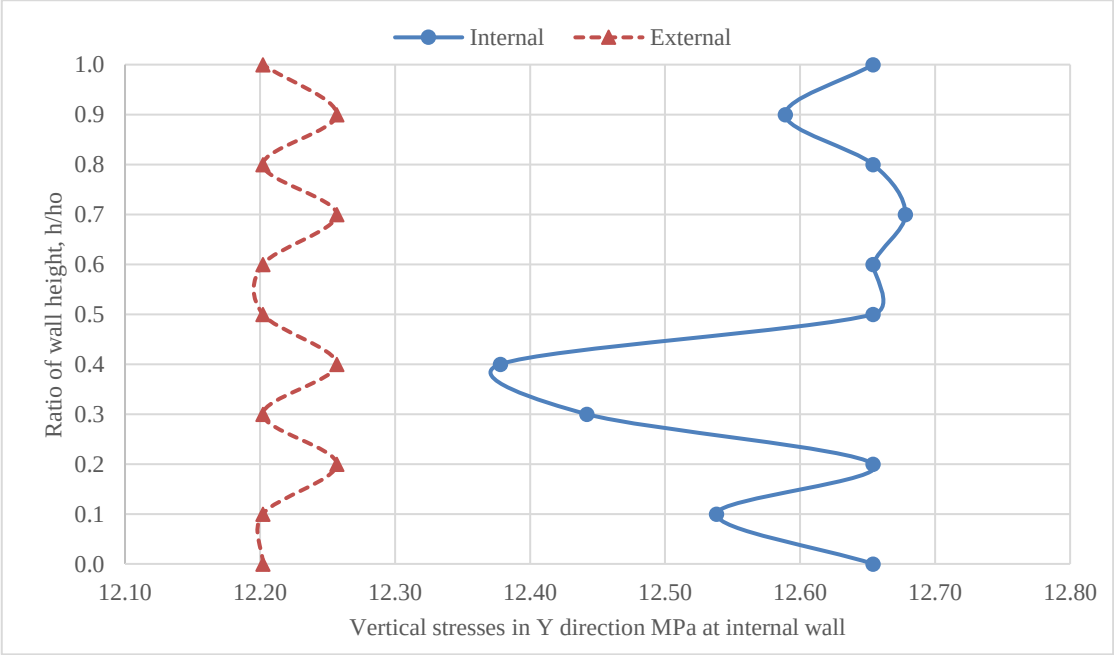

Figure 12: Mortar vertical stresses in the y-direction at internal and external walls.

6. Conclusion

A 2D model consists of three URM walls supporting RC slab has been simulated. The three URM walls were simulated with pure tensional potential cracks located vertically in the middle of mortar and units. The failure pressure of the simulated model was 1.327 MPa. The failure pressure represents the ultimate condition and has to be divided by a safety factor before comparing the results with masonry code. A safety factor equals to 1.5 is considered. The allowable load from the numerical analysis equals 0.885 MPa. A comparison has been conducted with the building code. According to Table 5.4.2 in the code, the allowable compressive stress on the gross cross-sectional area is 0.807 MPa. Hence, the code is conservative by about 10% compared to the simulated model even though cracks in masonry units and mortar joints have been simulated.

References

[1] Thomas, J. (2004). Effect of plastering on the out-of-plane flexural strength of single Wythe masonry wallets. Proceedings of the First CUSAT National Conference on Recent Advances in Civil Engineering, (pp. 144–149). Kochi, India.

[2] Laurenco, P. B., Rots, J. G., & Blaauwendraad, J. (1995). Two approaches for the analysis of masonry structures: micro and macro-modeling. HERON, 40 (4), 1995. Rots J. G. "Numerical simulation of cracking in structural masonry", HERON journal, 36(2), 1991, pages 49-63.

[3] Page, A. W. (1996). Unreinforced masonry structures-an Australian overview. Bulletin-New Zealand national society for earthquake engineering, 29, 242-255.

[4] Lourenço, P. B. (2013). Computational strategies for masonry structures: multi-scale modeling, dynamics, engineering applications, and other challenges. In Congreso de Métodos Numéricos en Ingeniería (pp. 1-17). Semni.

[5] Feba, S. T., & Kuriakose, B. (2017). Nonlinear Finite Element Analysis of Unreinforced Masonry Walls. In Applied Mechanics and Materials (Vol. 857, pp. 142-147). Trans Tech Publications.

[6] Rots, J. G. (1991). Numerical simulation of cracking in structural masonry. Heron, 36(2), 49-63.
[7] Marques, R., & Lourenço, P. B. (2011). Possibilities and comparison of structural component models for the seismic assessment of modern unreinforced masonry buildings. Computers & Structures, 89(21-22), 2079-2091.
[8] Singh, S. B., & Munjal, P. (2017). Bond strength and compressive stress-strain characteristics of brick masonry. J. Build. Eng. 9, (pp. 10–16).
[9] Ravula., M. B., & Subramaniam, K. (2017). Experimental investigation of compressive failure in masonry brick assemblages made with soft brick. Mater. Struct. 50 (19), (pp. 1-11.).
[10] Balasubramanian, S. R., Maheswari, D., Cynthia, A., Rao, K. B., Prasad, M. A., Goswami, R., & Sivakumar, P. (2015). Experimental determination of statistical parameters associated with uniaxial compression behaviour of brick masonry. Curr. Sci. 109 (11), (pp. 2094–2102).
[11] Nagarajan, S., Viswanathan, S., & Ravi, V. (2014). Experimental approach to investigate the behaviour of brick masonry for different mortar ratios. Proceedings of the International Conference on Advances in Engineering and Technology, (pp. 586–592). Singapore.
[12] Gumaste, K. S., Rao, K., Reddy, B., & Jagadish, K. S. (2007). Strength and elasticity of brick masonry prisms and wallettes under compression. Mater. Struct. 40 (2), (pp. 241–253).
[13] Mohamad, G., Lourenço, P. B., & Roman, H. R. (2007). Mechanics of hollow concrete block masonry prisms under compression: review and prospects. Cem. Concr. Compos 29 (3), (pp. 181-192).
[14] Lourenço, P. B. (2014). Masonry Structures, Overview. Encyclopedia of Earthquake Engineering, 1-9.
[15] Lourenço, P. B. (2002). Computations on historic masonry structures. Progress in Structural Engineering and Materials, 4(3), 301-319.
[16] Antonio Maria D'Altri, Stefano de Miranda, Giovanni Castellazzi, & Vasilis Sarhosis (2018). A 3D detailed micro-model for the in-plane and out-of-plane numerical analysis of masonry panels. Computers and Structures, Elsevier.
[17] Hongxue Han, Maurice Dusseault, Baoci Xu, & Bo Peng (2006). Simulation of Tectonic Deformation and Large Area Casing Shear Mechanisms-Part B: Geomechanics. American Rock Mechanics Association, ARMA/USRMS 06-1004. Golden, Colorado.
[18] Lourenço, P. B., & Rots, J. G. (1997). Multi-surface interface model for analysis of masonry structures. Journal of engineering mechanics, 123(7), 660-668.
[19] Ammar Rafid Ahmed, Alaa H. Al-Zuhairi, "Behavior of Clay Masonry Prism Under Vertical Load Using Detailed Micro Modeling Approach.", Arab Universities Union Journal. No. 3, 2019.
[20] Mohamad, G., Lourenço, P. B., Rizzatti, E., Roman, H. R., & Nakanishi, E. Y. (2012). Failure mode, deformability and strength of masonry walls. In 15th International Brick and Block Masonry Conference (pp. 1-12). Universidad Federal de Santa Catarina (UFSC).
[21] MSJC, (2011). Specification for Masonry Structures TMS 602-11/ ACI 530.1-11 / ASCE 6-11.